Letter Editors' Suggestion

Two-photon-interaction effects in the bad-cavity limit

Nicolò Piccione [1,*] Simone Felicetti,[2,3] and Bruno Bellomo[1]

[1] Institut UTINAM, CNRS UMR 6213, Université Bourgogne Franche-Comté, Observatoire des Sciences de l'Univers THETA, 41 bis avenue de l'Observatoire, F-25010 Besançon, France

[2] Istituto di Fotonica e Nanotecnologie, Consiglio Nazionale delle Ricerche, Piazza Leonardo da Vinci 32, I-20133 Milano, Italy

[3] Université de Paris, Laboratoire Matériaux et Phénomènes Quantiques, Centre National de la Recherche Scientifique, F-75013 Paris, France

(Received 15 July 2020; accepted 15 December 2021; published 26 January 2022)

Various experimental platforms have proven to be valid testbeds for the implementation of nondipolar light-matter interactions, where atomic systems and confined modes interact via two-photon couplings. Here, we study a damped quantum harmonic oscillator interacting with N two-level systems via a two-photon coupling in the so-called bad-cavity limit, in the presence of finite-temperature baths and coherent and incoherent drivings. We have succeeded in applying a recently developed adiabatic elimination technique to derive an effective master equation for the two-level systems, presenting two fundamental differences compared to the case of a dipolar interaction: an enhancement of the two-level systems spontaneouslike emission rate, including a thermal contribution and a quadratic term in the coherent driving, and an increment of the effective temperature perceived by the two-level systems. These differences give rise to striking effects in the two-level systems dynamics, including a faster generation of steady-state coherence and a richer dependence on temperature of the collective effects, which can be made stronger at higher temperature.

DOI: 10.1103/PhysRevA.105.L011702

I. INTRODUCTION

Atomic systems interacting with confined photonic or phononic modes represent one of the most studied classes of quantum-optical systems. On the one hand, the confinement may induce modifications of single atom absorption and emission rates such as the well-known Purcell effect [1]. On the other hand, the collective nature of such interactions gives rise to a rich quantum phenomenology characterized, for example, by the emergence of quantum phase transitions [2] and by the qualitative modifications of optical properties [3]. Concerning the latter, a sub- and a superradiant regime have been identified, respectively, characterized by the dampening or the amplification of atomic absorption and emission rates with respect to the independent-emitter case [4]. These regimes have been extensively studied also in the presence of coherent or incoherent optical drivings [5–12]. Much attention has been devoted to the so-called bad-cavity limit in which the confined mode is strongly dampened with respect to the interaction with the atoms [5–8,10,11]. In this context, the effective dynamics of the atoms can be obtained by adiabatically eliminating the confined mode [13–16].

Besides the fundamental interest, collective quantum phenomena induced by light-matter interactions can be exploited in a variety of applications. In particular, the sub- and superradiant regimes may be associated to the generation of collective states of the emitters, which are of great interest for quantum sensing [17,18], generation of nonclassical states [19], photon storage [20], and excitation transfer [21]. This phenomenology is of high experimental relevance, as collective light-matter interactions can be controllably implemented in a broad range of atomic and solid-state quantum systems, such as cold atoms [22], trapped ions [23], metamaterials [24], plasmonic cavities [25], color centres in diamonds [26], quantum dots [27], and superconducting circuits [28].

To the best of our knowledge, collective radiative phenomena have not so far been analyzed for two-photon (2ph) interactions. However, it has been recently predicted that using atomic or solid-state systems it is possible to implement nondipolar light-matter couplings, where the linear interaction is inhibited and where quantum emitters and localized bosonic modes interact via the exchange of two excitation quanta. In particular, such two-photon couplings can be observed by engineering superconducting atom-resonator systems [29,30] or by applying analog quantum simulation schemes in trapped ions [31–33] or ultracold atoms [34,35]. Notice that nondipolar transitions have already been observed using superconducting artificial atoms [36], and that quantum-simulation techniques have already been experimentally applied to observe the physics of fundamental dipolar light-matter interaction models in extreme regimes of parameters [35,37]. On the dissipative side, two-photon relaxation [38,39] and pumping [38] have also been theoretically analyzed and experimentally implemented [40]. The fast-growing interest in two-photon couplings is motivated by a rich phenomenology, characterized by counterintuitive spectral features [41–46], high-order quantum optical nonlinearities [29,30,47], and quantum phase transitions [48–52]. In turn, this phenomenology can be exploited in different quantum-information applications [53–55]. We finally stress that the two-photon coupling analyzed here differs from other physical situations for which the term "two-photon" is used. Some examples are two-photon excitations (see chapter 6.7 of

*nicolo.piccione@univ-fcomte.fr

Ref. [56]), two-photon absorption [57], two-plasmon emission [58], and two-photon emission coming from strong light-matter coupling [59].

In this Letter, we study the dynamics of a damped harmonic oscillator (HO) interacting with an ensemble of two-level systems (TLSs) in the bad-cavity limit in the case of a two-photon coupling. By applying a recently developed approach to perform adiabatic elimination in open quantum systems [15,16], we derive an effective master equation for the TLSs that takes into account the coupling with finite-temperature baths as well as coherent and incoherent optical drivings. Our analytical and numerical analysis of the time evolution and steady-state behavior unveils an unexpected collective phenomenology induced by nondipolar light-matter interactions. Compared to the dipolar case, the two-photon coupling introduces the possibility to enhance the absorption and emission processes, and leads to a higher resilience of sub- and superradiance with respect to the baths temperature.

II. PHYSICAL MODELS

We study a system composed of a damped HO interacting via a resonant Jaynes-Cummings Hamiltonian with N TLSs in the bad-cavity limit [13,14,16], comparing the one-photon (1ph) and 2ph interaction cases. The two models are described by the Hamiltonians

$$H_l = \hbar\omega a^\dagger a + \frac{l\hbar\omega}{2}J_z + \hbar g[a^l J_+ + (a^\dagger)^l J_-], \tag{1}$$

where $l = 1$ for the 1ph case and $l = 2$ for the 2ph one, ω is the frequency of the HO and $l\omega$ the one of the TLSs (i.e., we consider a resonant interaction in both cases), g is the coupling parameter between the HO and the TLSs, a and $a^\dagger$ are the usual annihilation and creation operators of a HO, while $J_z = \sum_{i=1}^N \sigma_z^{(i)}$ and $J_\pm = \sum_{i=1}^N \sigma_\pm^{(i)}$, where σ_z, σ_-, and σ_+ are, respectively, the z-Pauli, the lowering, and the raising operators of a TLS. The ground and the excited energy levels of each TLS are indicated, respectively, by $|g\rangle$ and $|e\rangle$. In Sec. I of the Supplemental Material (SM) [60] we provide an example of a possible implementation with superconducting circuits [61] of the above Hamiltonian for the case $l = 2$, by generalizing the study done in Ref. [30] to the case of more than one TLS.

We suppose that the HO and each TLS are each in contact with an independent thermal bath at temperature T (equal for all baths) and that a resonant coherent pumping on the HO and an incoherent local pumping on the TLSs are available. In the interaction picture, using a phenomenological approach [62–64], the master equation for the global density matrix ρ_G is

$$\dot\rho_G = -ig[a^l J_+ + (a^\dagger)^l J_- \rho_G] + \mathcal{L}_{\rm HO}(\rho_G) + \mathcal{L}_Q(\rho_G), \tag{2}$$

where $\mathcal{L}_{\rm HO}(\bullet)$ and $\mathcal{L}_Q(\bullet)$ are dissipators acting, respectively, on the HO and on the TLSs, given by

$$\begin{aligned}\mathcal{L}_{\rm HO}(\bullet) = &-i[(\beta^* a + \beta a^\dagger), \bullet]\\ &+ k[(1+\bar n_{\omega,T})\mathcal{D}_a(\bullet) + \bar n_{\omega,T}\mathcal{D}_{a^\dagger}(\bullet)],\\ \mathcal{L}_Q(\bullet) = &\sum_{i=1}^N \big[\gamma_{\rm loc}(1+\bar n_{l\omega,T})\mathcal{D}_{\sigma_-^{(i)}}(\bullet)\\ &+ (\gamma_{\rm loc}\bar n_{l\omega,T} + P)\mathcal{D}_{\sigma_+^{(i)}}(\bullet)\big],\end{aligned} \tag{3}$$

where $\mathcal{D}_X(\bullet) = X\bullet X^\dagger - \frac{1}{2}\{X^\dagger X, \bullet\}$, k and $\gamma_{\rm loc}$ are the relaxation rates of, respectively, the HO and each TLS due to the local couplings with their own thermal baths ($\gamma_{\rm loc}$ is assumed to be the same for all the TLSs), β characterizes the interaction between the HO and the coherent field, P quantifies the action of the incoherent pumping on each TLS, and $\bar n_{\omega,T} = [e^{\hbar\omega/(k_B T)} - 1]^{-1}$, k_B being the Boltzmann constant. The coherent pumping is treated in the rotating-wave approximation, being $|\beta| \ll \omega$. The phenomenological approach is justified because we consider the TLSs and the HO weakly coupled ($g \ll \omega$) [62], the HO weakly coupled to its bath ($k \ll \omega$) [62], and the external coherent field resonant with the HO [63].

III. ADIABATIC ELIMINATION

By applying a recently introduced adiabatic elimination technique [15,16] we have been able to derive an effective master equation for the reduced density matrix of the TLSs, $\rho = {\rm Tr}_{\rm HO}\{\rho_G\}$ (see Secs. II and III of SM [60] for a review of this technique, the detailed derivation, and some comments on the validity range of the adiabatic elimination):

$$\begin{aligned}\dot\rho = &-ig[\alpha^l J_+ + (\alpha^*)^l J_-, \rho] + \mathcal{L}_Q(\rho)\\ &+ \gamma_l[n_l\mathcal{D}_{J_+}(\rho) + (1+n_l)\mathcal{D}_{J_-}(\rho)],\end{aligned} \tag{4}$$

where we recall that $l = 1$ for the 1ph case and $l = 2$ for the 2ph one, and

$$\begin{aligned}&\alpha = -\frac{2i\beta}{k}, \quad \gamma_1 = \frac{4g^2}{k}, \quad n_1 = \bar n_{\omega,T},\\ &\gamma_2 = \gamma_1(1 + 2n_1 + 4|\alpha|^2),\\ &n_2 = n_1\frac{n_1 + 4|\alpha|^2}{1 + 2n_1 + 4|\alpha|^2}.\end{aligned} \tag{5}$$

As expected, even in the 2ph case the adiabatic elimination gives rise to collective dissipative terms [second line of Eq. (4)]. We observe that differently from the case of collective radiative phenomena induced by the interaction of different atoms with a common vacuum field [4], here the collective phenomena result from the coupling with a common damped HO. Notice that, although Eq. (4) retains its formal structure when changing l (see Sec. IV of SM [60] for details), the effective parameters α^l, γ_l, and n_l coming from the adiabatic elimination depend differently in the two models on the physical parameters g, β, k, ω, and T [see Eq. (5)]. This results in profound physical differences between the 1ph case and the 2ph one, leading to unexpected effects specific to the 2ph case. In particular, we can identify three main modifications. A first evident difference regards the dependence of the unitary driving term on α, which is linear in the 1ph case and quadratic in the 2ph one. An even more striking difference concerns the collective relaxation rate γ_l which, only in the 2ph case, depends on the parameters characterizing the state of the HO at order zero, n_1 and α (see Sec. III of the SM [60]). Finally, the coherent pumping increases the temperature of the effective collective bath seen by the TLSs, generated by the adiabatic elimination of the HO. In particular, setting $n_2 = \bar n_{2\omega,T^*} = [e^{2\hbar\omega/(k_B T^*)} - 1]^{-1}$, the temperature of this col-

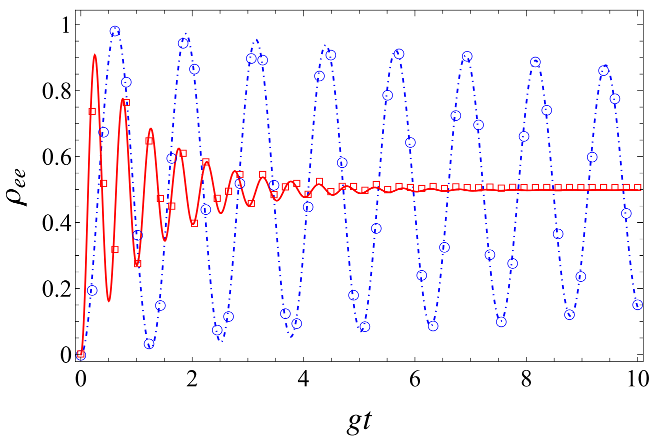

FIG. 1. Time evolution of the excited-state population of one TLS, ρ_{ee}, with physical parameters $\beta = 1.25k$ (so that $|\alpha| = 2.5$), $\gamma_{\rm loc} = 0$, $g = 0.01k$, $T = 0$, and $P = 0$. The dot-dashed blue line and the continuous red line are the curves obtained by using the effective model of Eq. (4) for, respectively, the 1ph and 2ph models. Empty markers show discrete points obtained from the numerical simulation of the full model of Eq. (2). In the 2ph model the steady state is clearly reached much faster.

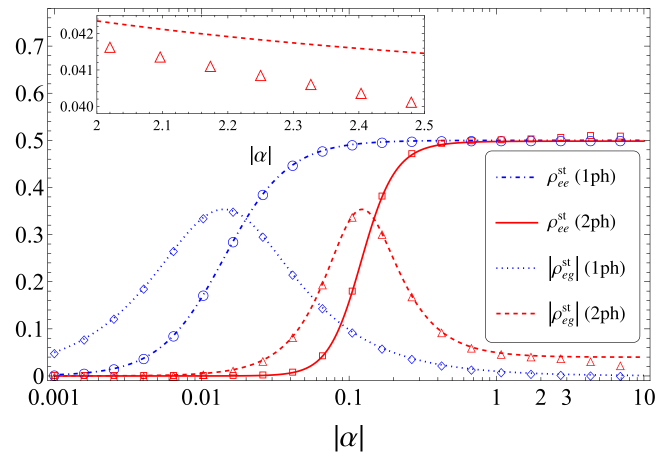

FIG. 2. Steady-state excited populations and coherences of one TLS as a function of $|\alpha|$ with $\gamma_{\rm loc} = 0$, $g = 0.01k$, $T = 0$, and $P = 0$. The various empty markers show discrete points computed with the full model of Eq. (2). As predicted, the error induced by the effective model increases as $|\alpha|$ increases. The inset shows a zoom of the 2ph steady-state coherence for $2 \leqslant |\alpha| \leqslant 2.5$. Both the full and the effective model predict a very low variation of the coherence in this range of $|\alpha|$.

lective bath is

$$T^* = \frac{2\hbar\omega}{k_B}\left[\ln\left(\frac{e^{2\hbar\omega/(k_BT)} - 2}{1 + 4|\alpha|^2(e^{\hbar\omega/(k_BT)} - 1)} + 2\right)\right]^{-1}. \quad (6)$$

Notice that when $\alpha = 0$ the temperature of this collective bath would be the same as that of the original bath of the HO ($T^* = T$). The peculiar form of γ_2 and n_2, especially their quadratic dependence on $|\alpha|$, can be useful to manipulate the dynamics of the TLSs, possibly enhancing their absorption and emission processes.

In the following, we discuss the physical consequences of these differences. In order to check the validity of the adiabatic elimination, we will show in several figures numerical simulations of the full model of Eq. (2).

IV. COHERENT DRIVING EFFECTS: FASTER DYNAMICS AND ROBUST STEADY-STATE COHERENCE

In order to focus on the effects due to the coherent pumping on the HO, let us consider the case of zero temperature and no local incoherent pumping on the TLSs. For $T = 0$ and $P = 0$, Eq. (4) simplifies and $\gamma_2 = \gamma_1(1 + 4|\alpha|^2)$.

The quadratic dependence of γ_2 on $|\alpha|$ can be exploited to make the system reach much faster its steady state in the 2ph case. This is shown in Fig. 1, comparing the dynamics of one TLS (henceforth we use the notation $\langle x|\rho|y\rangle = \rho_{xy}$) for the two models.

Focusing on the reachable steady states $\rho^{\rm st}$ in the one TLS case, Fig. 2 shows that nondiagonal ones in the bare basis, that is, those presenting coherences, can be obtained. The analytical expression of these coherences in the general case ($T \neq 0$ and $P \neq 0$) can be found in Sec. V A of the SM [60]. In particular, non-negligible coherences are obtained when g is sufficiently high (but inside the validity range of the adiabatic elimination). By comparing the two models, one can see that great differences arise for $|\alpha| \gtrsim 1$. In this regime, indeed, the 2ph interaction allows one to generate steady states in much shorter time (as one can evince from Fig. 1) and with higher coherences. Moreover, the steady state does not change much for little variations of $|\alpha|$ when $|\alpha|$ is high enough. This is due to the fact that when $\gamma_{\rm loc}$ is negligible, the steady state depends only on the ratio $\gamma_l/(g|\alpha|^l)$, which in the 2ph case does not tend to zero but to $16g/k$. For example, when $\gamma_{\rm loc} = 0$ and $g = 0.01k$, the steady-state coherences for $2 \leqslant |\alpha| \leqslant 2.5$ are very close, as shown in the inset of Fig. 2. Therefore, it is possible to rapidly generate nondiagonal steady states resilient to intensity fluctuations of the coherent driving. We stress that the generation of steady-state coherence is relevant since, in general, it is considered as a resource for quantum technologies [65]. In particular, it has been recently shown that nondiagonal steady states can find applications in quantum metrology protocols [66,67], which could be then enhanced by generating these states faster.

V. TEMPERATURE RESILIENCE OF COLLECTIVE PHENOMENA

Let us now consider the case of no coherent pumping, in order to focus on the emergence of correlations due to the collective dissipative terms. For $\alpha = 0$, in Eq. (4) the unitary term disappears, $\gamma_2 = \gamma_1(1 + 2n_1)$, and $n_2 = n_1^2/(1 + 2n_1) = 1/[e^{2\hbar\omega/(k_BT)} - 1]$. This particular setting has been used [7,8] to study the emergence of sub- and superradiant steady states as a function of the incoherent pumping parameter P when $T = 0$. The quantity $J_{\rm corr} = \langle J_+J_-\rangle - \sum_{i=1}\langle\sigma_+^{(i)}\sigma_-^{(i)}\rangle$ is used to characterize these collective phenomena. In particular, $J_{\rm corr} > 0$ indicates the occurrence of superradiance while $J_{\rm corr} < 0$ indicates that of subradiance.

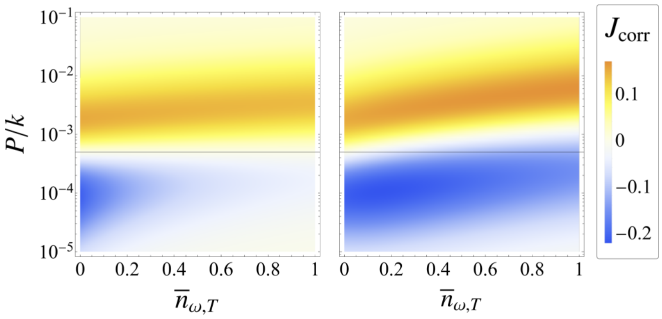

FIG. 3. J_{corr} of the steady state of two TLSs as a function of T ($\bar{n}_{\omega,T}$ in the plot) and P/k in the 1ph and 2ph cases for $g = 0.01k$, $\gamma_{loc} = 10^{-4}k$, and $\alpha = 0$. The horizontal lines correspond to the value $P = P^* \equiv \gamma_{loc} + \gamma_1 = 5 \times 10^{-4}k$, where both models give exactly $J_{corr} = 0$ at zero temperature. The 2ph model exhibits a richer dependence on temperature including stronger subradiance and superradiance at higher temperatures. Note that the extremal values that J_{corr} may assume in the two-TLS case are −1 and 1.

When $T = 0$, there is no difference between the 1ph and the 2ph models because $\gamma_2 = \gamma_1$. In contrast, the two models behave very differently for $T \neq 0$, as shown in Fig. 3 where we plot the steady value of J_{corr} in the two models as functions of the incoherent pumping and the baths temperature in the case of two TLSs, for $g = 0.01k$ and $\gamma_{loc} = 10^{-4}k$. A more varied dependence of the collective phenomena on temperature in the 2ph case is observed due to the increase of the collective dissipation rate γ_2 with the temperature. In particular, remarkable differences are observed when P is close to $P^* \equiv \gamma_1 + \gamma_{loc}$, since for this value of P, in the 1ph case, $J_{corr} = 0$ for any T, while this is not the case in the 2ph case. This can be also evinced by the analytical expression we have obtained for J_{corr} in the two-TLS case (see Sec. V B of the SM [60]) which shows that subradiance and superradiance are obtained when P is, respectively, lower or higher than $\gamma_l + \gamma_{loc}$. This behavior of the sign of J_{corr} has been confirmed in all the other simulations that we have done (up to six TLSs). This means that for $P = P^*$, since γ_2 increases with temperature, subradiance is observed for any temperature different from zero in the 2ph case. One could wonder if part of these differences arises just because the TLSs in the 2ph model have frequency 2ω so that, for the same temperature, they interact with local baths by means of a lower average excitation number. To check the extent of this effect we have also looked at the same plot using the frequency 2ω for the TLSs and the HO for the 1ph case finding only a partial reduction of the differences between the two models. An example of this issue is treated for a specific example in Fig. 4.

A different behavior of collective phenomena is still present in the case of a larger number of TLSs, as exhibited in Fig. 4(a), where the plot of J_{corr} in the steady state as a function of the incoherent pumping for four TLSs at a fixed temperature ($\bar{n}_{\omega,T} = 1$) clearly shows relevant differences in the two models, especially for the subradiance. In particular, in the 2ph case, a higher peak of both super- and subradiance can be reached, even when the frequency of the TLSs and of the HO in the 1ph case is set equal to 2ω. A more striking different behavior of the two models can be obtained by studying

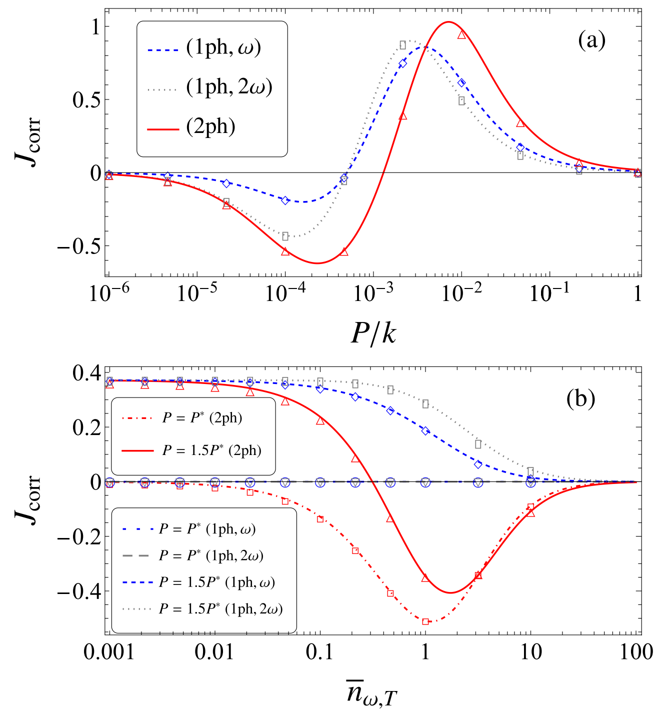

FIG. 4. (a) J_{corr} of the steady state of four TLSs as a function of P, for $g = 0.01k$, $\gamma_{loc} = 10^{-4}k$, T such that $\bar{n}_{\omega,T} = 1$, and $\alpha = 0$. Here, J_{corr} is plotted for the 1ph (for both ω and 2ω) and 2ph cases. (b) Steady J_{corr} of four TLSs as a function of T ($\bar{n}_{\omega,T}$ in the plot), for $g = 0.01k$, $\gamma_{loc} = 10^{-4}k$, and $\alpha = 0$, for $P = P^* \equiv \gamma_{loc} + \gamma_1 = 5 \times 10^{-4}k$ and $P = 1.5P^*$ (see legend). The 1ph (ω and 2ω) and 2ph cases are compared. In both plots, J_{corr} is always zero for $P = P^*$ in the 1ph case and the various empty markers indicate discrete points computed with the full model of Eq. (2), i.e., without performing the adiabatic elimination [in panel (b), because of computational difficulties only points with $\bar{n}_{\omega,T}$ up to 10 are considered]. Note that the extremal values that J_{corr} may assume in the four-TLS case are −2 and 4.

the dependence of the steady value of J_{corr} on T for specific values of the pump, as shown in Fig. 4(b). For $P = P^*$ no subradiance nor superradiance is visible in the 1ph case, while in the 2ph case a strong subradiance may be observed. An even more interesting case is obtained for $P > P^*$. In this case, the system displays superradiance at $T = 0$ in both models while it follows very different paths, depending on the model, when the temperature increases. In the 1ph model, J_{corr} is always positive and tends to zero for increasing temperature whereas, in the 2ph model, there is a temperature T' such that $P < \gamma_2 + \gamma_{loc}$ for $T > T'$. Therefore, in the 2ph model, the system can go into a subradiant zone inaccessible through the 1ph interaction at fixed pumping.

VI. CONCLUSIONS

In summary, we have studied the case of a damped HO interacting with N TLSs via a two-photon coupling in the bad-cavity limit in the presence of finite temperature baths, a coherent pumping on the HO, and an incoherent pumping on the TLSs, comparing it to the one-photon-coupling case. We have succeeded in applying a recent adiabatic elimination technique in the two-photon model to derive a master equation governing the collective evolution of the TLSs. This presents two fundamental differences compared to the dipolar case: an enhancement of the spontaneouslike emission rate, including a thermal contribution and a quadratic term in the coherent driving, and an increased temperature of the effective bath experienced by the TLSs. This unexpected phenomenology makes it possible to accelerate the generation of nondiagonal one-TLS steady states and to observe a drastic change of the temperature-dependent behavior of quantum collective phenomena, leading to a stronger resilience of these phenomena to high temperatures. We finally remark that the models here investigated can be feasibly implemented with both solid-state and atomic existing quantum technologies, as also discussed in Sec. I of SM [60] for the 2ph model in the solid-state context.

ACKNOWLEDGMENTS

N.P. acknowledges the financial support of the Observatoire des Sciences de l'Univers THETA Franche-Comté / Bourgogne for his research visit at the Université Paris Diderot (now Université de Paris). B.B. acknowledges support by the French "Investissements d'Avenir" program, project ISITE-BFC (Contract No. ANR-15-IDEX-03). N.P. and B.B. thank Andrea Smirne for useful discussions about the results of this Letter.

[1] S. Haroche and J.-M. Raimond, *Exploring The Quantum: Atoms, Cavities, and Photons* (Oxford University, New York, 2006).

[2] P. Kirton, M. M. Roses, J. Keeling, and E. G. Dalla Torre, Introduction to the Dicke Model: From equilibrium to nonequilibrium, and vice versa, Adv. Quantum Technol. **2**, 1800043 (2019).

[3] M. G. Benedict, *Super-Radiance: Multiatomic Coherent Emission* (CRC, Boca Raton, FL, 1996).

[4] M. Gross and S. Haroche, Superradiance: An essay on the theory of collective spontaneous emission, Phys. Rep. **93**, 301 (1982).

[5] D. Meiser, J. Ye, D. R. Carlson, and M. J. Holland, Prospects for a Millihertz-Linewidth Laser, Phys. Rev. Lett. **102**, 163601 (2009).

[6] D. Meiser and M. J. Holland, Steady-state superradiance with alkaline-earth-metal atoms, Phys. Rev. A **81**, 033847 (2010).

[7] D. Meiser and M. J. Holland, Intensity fluctuations in steady-state superradiance, Phys. Rev. A **81**, 063827 (2010).

[8] A. Auffèves, D. Gerace, S. Portolan, A. Drezet, and M. F. Santos, Few emitters in a cavity: From cooperative emission to individualization, New J. Phys. **13**, 093020 (2011).

[9] N. Shammah, N. Lambert, F. Nori, and S. De Liberato, Superradiance with local phase-breaking effects, Phys. Rev. A **96**, 023863 (2017).

[10] P. Kirton and J. Keeling, Superradiant and lasing states in driven-dissipative Dicke models, New J. Phys. **20**, 015009 (2018).

[11] N. Shammah, S. Ahmed, N. Lambert, S. De Liberato, and F. Nori, Open quantum systems with local and collective incoherent processes: Efficient numerical simulations using permutational invariance, Phys. Rev. A **98**, 063815 (2018).

[12] F. Damanet, A. J. Daley, and J. Keeling, Atom-only descriptions of the driven-dissipative Dicke model, Phys. Rev. A **99**, 033845 (2019).

[13] R. Bonifacio, P. Schwendimann, and F. Haake, Quantum statistical theory of superradiance. I, Phys. Rev. A **4**, 302 (1971).

[14] R. Bonifacio, P. Schwendimann, and F. Haake, Quantum statistical theory of superradiance. II, Phys. Rev. A **4**, 854 (1971).

[15] R. Azouit, F. Chittaro, A. Sarlette, and P. Rouchon, Towards generic adiabatic elimination for bipartite open quantum systems, Quantum Sci. Technol. **2**, 044011 (2017).

[16] R. Azouit, Adiabatic elimination for open quantum systems, Ph.D. thesis, PSL Research University, 2017.

[17] I. D. Leroux, M. H. Schleier-Smith, and V. Vuletić, Implementation of Cavity Squeezing of a Collective Atomic Spin, Phys. Rev. Lett. **104**, 073602 (2010).

[18] G. Tóth and I. Apellaniz, Quantum metrology from a quantum information science perspective, J. Phys. A **47**, 424006 (2014).

[19] F. Jahnke, C. Gies, M. Aßmann, M. Bayer, H. Leymann, A. Foerster, J. Wiersig, C. Schneider, M. Kamp, and S. Höfling, Giant photon bunching, superradiant pulse emission and excitation trapping in quantum-dot nanolasers, Nat. Commun. **7**, 11540 (2016).

[20] A. Asenjo-Garcia, M. Moreno-Cardoner, A. Albrecht, H. J. Kimble, and D. E. Chang, Exponential Improvement in Photon Storage Fidelities Using Subradiance and "Selective Radiance" in Atomic Arrays, Phys. Rev. X **7**, 031024 (2017).

[21] F. J. Garcia-Vidal and J. Feist, Long-distance operator for energy transfer, Science **357**, 1357 (2017).

[22] A. Goban, C.-L. Hung, J. D. Hood, S.-P. Yu, J. A. Muniz, O. Painter, and H. J. Kimble, Superradiance for Atoms Trapped along a Photonic Crystal Waveguide, Phys. Rev. Lett. **115**, 063601 (2015).

[23] R. G. DeVoe and R. G. Brewer, Observation of Superradiant and Subradiant Spontaneous Emission of Two Trapped Ions, Phys. Rev. Lett. **76**, 2049 (1996).

[24] S. D. Jenkins, J. Ruostekoski, N. Papasimakis, S. Savo, and N. I. Zheludev, Many-Body Subradiant Excitations in Metamaterial Arrays: Experiment and Theory, Phys. Rev. Lett. **119**, 053901 (2017).

[25] V. N. Pustovit and T. V. Shahbazyan, Cooperative Emission of Light by an Ensemble of Dipoles Near a Metal Nanoparticle: The Plasmonic Dicke Effect, Phys. Rev. Lett. **102**, 077401 (2009).

[26] A. Angerer *et al.*, Superradiant emission from colour centres in diamond, Nat. Phys. **14**, 1168 (2018).

[27] M. Scheibner, T. Schmidt, L. Worschech, A. Forchel, G. Bacher, T. Passow, and D. Hommel, Superradiance of quantum dots, Nat. Phys. **3**, 106 (2007).

[28] J. A. Mlynek, A. A. Abdumalikov, C. Eichler, and A. Wallraff, Observation of Dicke superradiance for two artificial atoms in a cavity with high decay rate, Nat. Commun. **5**, 5186 (2014).

[29] S. Felicetti, D. Z. Rossatto, E. Rico, E. Solano, and P. Forn-Díaz, Two-photon quantum Rabi model with superconducting circuits, Phys. Rev. A **97**, 013851 (2018).

[30] S. Felicetti, M.-J. Hwang, and A. Le Boité, Ultrastrong-coupling regime of nondipolar light-matter interactions, Phys. Rev. A **98**, 053859 (2018).

[31] S. Felicetti, J. S. Pedernales, I. L. Egusquiza, G. Romero, L. Lamata, D. Braak, and E. Solano, Spectral collapse via two-phonon interactions in trapped ions, Phys. Rev. A **92**, 033817 (2015).

[32] X.-H. Cheng, I. Arrazola, J. S. Pedernales, L. Lamata, X. Chen, and E. Solano, Nonlinear quantum Rabi model in trapped ions, Phys. Rev. A **97**, 023624 (2018).

[33] R. Puebla, J. Casanova, O. Houhou, E. Solano, and M. Paternostro, Quantum simulation of multiphoton and nonlinear dissipative spin-boson models, Phys. Rev. A **99**, 032303 (2019).

[34] P. Schneeweiss, A. Dareau, and C. Sayrin, Cold-atom-based implementation of the quantum Rabi model, Phys. Rev. A **98**, 021801(R) (2018).

[35] A. Dareau, Y. Meng, P. Schneeweiss, and A. Rauschenbeutel, Observation of Ultrastrong Spin-Motion Coupling for Cold Atoms in Optical Microtraps, Phys. Rev. Lett. **121**, 253603 (2018).

[36] J. Goetz, F. Deppe, K. G. Fedorov, P. Eder, M. Fischer, S. Pogorzalek, E. Xie, A. Marx, and R. Gross, Parity-Engineered Light-Matter Interaction, Phys. Rev. Lett. **121**, 060503 (2018).

[37] D. Lv, S. An, Z. Liu, J.-N. Zhang, J. S. Pedernales, L. Lamata, E. Solano, and K. Kim, Quantum Simulation of the Quantum Rabi Model in a Trapped Ion, Phys. Rev. X **8**, 021027 (2018).

[38] F. Minganti, N. Bartolo, J. Lolli, W. Casteels, and C. Ciuti, Exact results for Schrödinger cats in driven-dissipative systems and their feedback control, Sci. Rep. **6**, 26987 (2016).

[39] M. Malekakhlagh and A. W. Rodriguez, Quantum Rabi Model with Two-Photon Relaxation, Phys. Rev. Lett. **122**, 043601 (2019).

[40] Z. Leghtas *et al.*, Confining the state of light to a quantum manifold by engineered two-photon loss, Science **347**, 853 (2015).

[41] I. Travěnec, Solvability of the two-photon Rabi Hamiltonian, Phys. Rev. A **85**, 043805 (2012).

[42] L. Duan, Y.-F. Xie, D. Braak, and Q.-H. Chen, Two-photon Rabi model: Analytic solutions and spectral collapse, J. Phys. A **49**, 464002 (2016).

[43] A. J. Maciejewski and T. Stachowiak, A novel approach to the spectral problem in the two photon Rabi model, J. Phys. A **50**, 244003 (2017).

[44] Y.-F. Xie, L. Duan, and Q.-H. Chen, Generalized quantum Rabi model with both one- and two-photon terms: A concise analytical study, Phys. Rev. A **99**, 013809 (2019).

[45] L. Cong, X.-M. Sun, M. Liu, Z.-J. Ying, and H.-G. Luo, Polaron picture of the two-photon quantum Rabi model, Phys. Rev. A **99**, 013815 (2019).

[46] R. J. Armenta Rico, F. H. Maldonado-Villamizar, and B. M. Rodriguez-Lara, Spectral collapse in the two-photon quantum Rabi model, Phys. Rev. A **101**, 063825 (2020).

[47] F. Zou, X.-Y. Zhang, X.-W. Xu, J.-F. Huang, and J.-Q. Liao, Multiphoton blockade in the two-photon Jaynes-Cummings model, Phys. Rev. A **102**, 053710 (2020).

[48] L. Garbe, I. L. Egusquiza, E. Solano, C. Ciuti, T. Coudreau, P. Milman, and S. Felicetti, Superradiant phase transition in the ultrastrong-coupling regime of the two-photon Dicke model, Phys. Rev. A **95**, 053854 (2017).

[49] X.-Y. Chen and Y.-Y. Zhang, Finite-size scaling analysis in the two-photon Dicke model, Phys. Rev. A **97**, 053821 (2018).

[50] S. Cui, F. Hébert, B. Grémaud, V. G. Rousseau, W. Guo, and G. G. Batrouni, Two-photon Rabi-Hubbard and Jaynes-Cummings-Hubbard models: Photon-pair superradiance, Mott insulator, and normal phases, Phys. Rev. A **100**, 033608 (2019).

[51] L. Garbe, P. Wade, F. Minganti, N. Shammah, S. Felicetti, and F. Nori, Dissipation-induced bistability in the two-photon Dicke model, Sci. Rep. **10**, 13408 (2020).

[52] S. Cui, B. Grémaud, W. Guo, and G. G. Batrouni, Nonlinear two-photon Rabi-Hubbard model: Superradiance, photon, and photon-pair Bose-Einstein condensates, Phys. Rev. A **102**, 033334 (2020).

[53] C. J. Villas-Boas and D. Z. Rossatto, Multiphoton Jaynes-Cummings Model: Arbitrary Rotations in Fock Space and Quantum Filters, Phys. Rev. Lett. **122**, 123604 (2019).

[54] J. Casanova, R. Puebla, H. Moya-Cessa, and M. B. Plenio, Connecting *n*th order generalised quantum Rabi models: Emergence of nonlinear spin-boson coupling via spin rotations, Npj Quantum Inf. **4**, 47 (2018).

[55] C. A. González-Gutiérrez and J. M. Torres, Atomic Bell measurement via two-photon interactions, Phys. Rev. A **99**, 023854 (2019).

[56] R. Loudon, *The Quantum Theory of Light* (Oxford University, New York, 2000).

[57] M. Rumi and J. W. Perry, Two-photon absorption: An overview of measurements and principles, Adv. Opt. Photon. **2**, 451 (2010).

[58] N. Rivera, I. Kaminer, B. Zhen, J. D. Joannopoulos, and M. Soljačić, Shrinking light to allow forbidden transitions on the atomic scale, Science **353**, 263 (2016).

[59] J. Flick, N. Rivera, and P. Narang, Strong light-matter coupling in quantum chemistry and quantum photonics, Nanophotonics **7**, 1479 (2018).

[60] See Supplemental Material at http://link.aps.org/supplemental/10.1103/PhysRevA.105.L011702 for a detailed description of a superconducting quantum circuit scheme implementing the 2ph model, a review of the recently developed adiabatic elimination technique and its application to the 1ph and 2ph cases, some details about the mapping between the 1ph and 2ph master equations, and steady-state formula for the one- and two-TLS cases.

[61] A. Blais, A. L. Grimsmo, S. M. Girvin, and A. Wallraff, Circuit quantum electrodynamics, Rev. Mod. Phys. **93**, 025005 (2021).

[62] H.-P. Breuer and F. Petruccione, *The Theory of Open Quantum Systems* (Oxford University, New York, 2007).

[63] Á. Rivas, A. D. K. Plato, S. F. Huelga, and M. B. Plenio, Markovian master equations: A critical study, New J. Phys. **12**, 113032 (2010).

[64] G. L. Giorgi, A. Saharyan, S. Guérin, D. Sugny, and B. Bellomo, Microscopic and phenomenological models of driven systems in structured reservoirs, Phys. Rev. A **101**, 012122 (2020).

[65] A. Streltsov, G. Adesso, and M. B. Plenio, *Colloquium*: Quantum coherence as a resource, Rev. Mod. Phys. **89**, 041003 (2017).

[66] Z. Wang, W. Wu, G. Cui, and J. Wang, Coherence enhanced quantum metrology in a nonequilibrium optical molecule, New J. Phys. **20**, 033034 (2018).

[67] A. Smirne, A. Lemmer, M. B. Plenio, and S. F. Huelga, Improving the precision of frequency estimation via long-time coherences, Quantum Sci. Technol. **4**, 025004 (2019).